© 2019. Published by The Company of Biologists Ltd | Development (2019) 146, dev170704. doi:10.1242/dev.170704

RESEARCH ARTICLE

Nell2 regulates the contralateral-versus-ipsilateral visual projection as a domain-specific positional cue

Chizu Nakamoto[1], Elaine Durward[1], Masato Horie[2] and Masaru Nakamoto[1,*]

ABSTRACT

In mammals with binocular vision, retinal ganglion cell (RGC) axons from each eye project to eye-specific domains in the contralateral and ipsilateral dorsal lateral geniculate nucleus (dLGN), underpinning disparity-based stereopsis. Although domain-specific axon guidance cues that discriminate contralateral and ipsilateral RGC axons have long been postulated as a key mechanism for development of the eye-specific retinogeniculate projection, the molecular nature of such cues has remained elusive. Here, we show that the extracellular glycoprotein Nell2 (neural epidermal growth factor-like-like 2) is expressed in the dorsomedial region of the dLGN, which ipsilateral RGC axons terminate in and contralateral axons avoid. In Nell2 mutant mice, contralateral RGC axons abnormally invaded the ipsilateral domain of the dLGN, and ipsilateral axons terminated in partially fragmented patches, forming a mosaic pattern of contralateral and ipsilateral axon-termination zones. *In vitro*, Nell2 exerted inhibitory effects on contralateral, but not ipsilateral, RGC axons. These results provide evidence that Nell2 acts as a domain-specific positional label in the dLGN that discriminates contralateral and ipsilateral RGC axons, and that it plays essential roles in the establishment of the eye-specific retinogeniculate projection.

KEY WORDS: Axon guidance, Retinogeniculate projection, Domain-specific guidance cue, Nel/Nell2, Mouse

INTRODUCTION

In his treatise on optics, Isaac Newton predicted that binocular vision would rely on the convergence of information from both eyes on the same site in the brain, and that a partial decussation of the optic nerve fibres would be necessary for binocular integration (Newton, 1730). His anatomical prediction was verified not long afterwards in dissections of the mammalian visual system (Pettigrew, 1986; Polyak, 1957). In mammals with good binocular vision, visual information from each eye is transferred to both sides of the brain via axons of retinal ganglion cells (RGCs): RGC axons from the nasal retina cross the midline at the optic chiasm and project to the contralateral side of the brain, whereas axons from a segment of the temporal retina project to the ipsilateral side. Ipsilaterally projecting RGCs localize in the defined retinal area of binocular overlap, and their number and distribution correlate with the extent of binocular vision and the orientation of the orbits (Heesy, 2004). In mice, ipsilateral RGC axons arise from a ventrotemporal segment of the retina and comprise ∼3-5% of the optic nerve fibres (Erskine and Herrera, 2014; Petros et al., 2008).

In the mammalian visual system, RGC axons project in an orderly manner to their main forebrain target: the dorsal lateral geniculate nucleus (dLGN) of the thalamus. The patterning of retinogeniculate axons involves: (1) segregation of right and left eye inputs; (2) topographic map formation; and (3) placement of eye-specific layers or domains that locate in stereotypic positions in the dLGN (Huberman et al., 2008; Pfeiffenberger et al., 2005). The precise targeting of RGC axons allows integration of visual information from both eyes in the brain, thus underpinning disparity-based stereopsis (depth perception and visual measurement of distance) (Wilks et al., 2013).

Spontaneous retinal activity has been thought to play crucial roles in eye-specific segregation of RGC axons in the dLGN (Huberman, 2007), and several molecules have been shown to play important roles in this activity-dependent segregation (Huh et al., 2000), including class I MHC (major histocompatibility complex), CD3ζ (Huh et al., 2000), neuronal pentraxins (Bjartmar et al., 2006), Zic2 and serotonin transporter (Sert) (Garcia-Frigola and Herrera, 2010).

Activity-dependent mechanisms, however, cannot account for the stereotypical locations of termination domains for contralateral and ipsilateral RGC axons within the dLGN (Huberman et al., 2002; Muir-Robinson et al., 2002). Previous studies have shown that expression gradients of ephrin A proteins across the dLGN, which play a key role in topographic mapping of the nasotemporal axis of the retina onto the dLGN, are also required for proper placement of eye-specific inputs in the dLGN (Huberman et al., 2005; Pfeiffenberger et al., 2005). Teneurin 3, another transmembrane protein expressed in a gradient in the dLGN, was also shown to regulate mapping of ipsilateral retinogeniculate projection (Leamey et al., 2007).

A relatively simple model that could explain the stereotypical placement of the eye-specific domains is that domain-specific positional cues, which can discriminate contralateral and ipsilateral RGC axons, guide incoming RGC axons to the correct eye-specific domains in the dLGN (Chapman, 2000; Crowley and Katz, 1999; Huberman et al., 2002; Shatz, 1996). However, the molecular nature of such domain-specific guidance cues has remained to be elucidated.

Nell2 (neural epidermal growth factor (EGF)-like-like 2; initially identified in the chick and named 'Nel') is an extracellular glycoprotein that has structural similarities with thrombospondin 1 and is predominantly expressed in the nervous system (Kuroda et al., 1999; Matsuhashi et al., 1995, 1996; Nelson et al., 2004, 2002; Oyasu et al., 2000; Watanabe et al., 1996). We have previously demonstrated that Nell2 acts as an inhibitory guidance cue for chick RGC axons *in vitro* (Jiang et al., 2009; Nakamura et al., 2012).

In this study, we have examined functions of Nell2 in the eye-specific retinogeniculate projection *in vivo* and in regulation of ipsilateral and contralateral RGC axon behaviour *in vitro*. Here, we

[1]Aberdeen Developmental Biology Group, School of Medicine, Medical Sciences and Nutrition, University of Aberdeen, Aberdeen AB25 2ZD, UK. [2]Department of CNS Research, Otsuka Pharmaceutical, 463-10 Kagasuno, Kawauchi-cho, Tokushima 771-0192, Japan.

*Author for correspondence (masanakamoto@hotmail.com)

C.N., 0000-0002-6560-3545; M.N., 0000-0001-9356-1189

Received 15 August 2018; Accepted 29 January 2019

Development (2019) 146, dev170704. doi:10.1242/dev.170704

show that Nell2 is expressed in the dorsomedial region of the dLGN, which corresponds to the territory receiving ipsilateral RGC axons. *In vivo* axon tracing analyses showed that the eye-specific pattern of the retinogeniculate projection was disrupted in Nell2 null (*Nell2*$^{-/-}$) mice: contralateral RGC axons abnormally invaded the ipsilateral domain of the dLGN, whereas ipsilateral axons terminated in partially fragmented patches, thus forming a mosaic pattern of contralateral and ipsilateral axon termination zones. *In vitro*, Nell2 inhibited outgrowth, induced growth cone collapse and caused repulsion in contralateral, but not ipsilateral, RGC axons. This contralateral axon-specific inhibition was observed both in wild-type and *Nell2*$^{-/-}$ RGCs. These results provide evidence that Nell2 acts as an inhibitory guidance molecule that is specific for contralateral RGC axons and prevents them from invading the ipsilateral territory of the dLGN. In addition, our findings indicate that a domain-specific positional label which exerts discriminatory effects on contralateral and ipsilateral axons plays essential roles in establishment of the eye-specific patterns in the visual system.

RESULTS

Nell2 expression domain overlaps with the ipsilateral domain of the dLGN

To explore potential functions of Nell2 in development of the eye-specific targeting patterns, we first examined Nell2 expression in the dLGN at the time of retinogeniculate projection by RNA *in situ* hybridization. In the mouse, first contralateral RGC axons enter the dLGN by embryonic day (E) 16, and ipsilateral axons around E18-birth (Godement et al., 1984). Nell2 expression was detected in the developing dLGN at E18.5 (Fig. 1A). Between postnatal day 1 (P1) and P10, by which the initial pattern of the retinogeniculate projection is established (Godement et al., 1984; Huberman et al., 2010), Nell2 expression levels increased and became restricted to the dorsomedial region of the dLGN, where ipsilateral RGC axons normally terminate (Fig. 1B-F). No obvious gradient of expression was observed for Nell2 in the dLGN (Flanagan, 2006). Nell2 expression in the dLGN appeared to be decreased and diffused after P12 (Fig. S1).

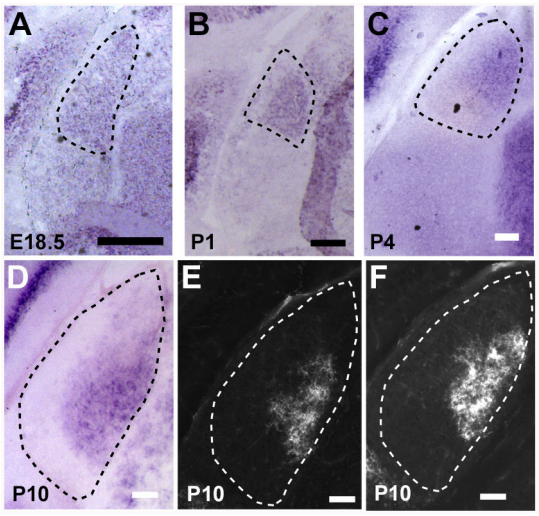

Fig. 1. Nell2 expression in the developing mouse dLGN. Coronal sections through the dLGN prepared from E18.5 (A), P1 (B), P4 (C) and P10 (D-F) mouse embryos are shown. Dorsal is at the top; lateral is on the left. Dotted lines indicate the boundary of the dLGN. (A-D) Sections were subjected to RNA *in situ* hybridization using a probe for Nell2. (E) Localization of the Nell2 protein was determined by immunohistochemistry using anti-Nell2 antibody. (F) Termination area of ipsilateral RGC axons in the dLGN at P10. RGC axons were labelled with cholera-toxin B (CTB)-Alexa Fluor at P7. Strong expression of Nell2 (RNA and protein) was detected in the dorsomedial region of the dLGN, which overlaps with the ipsilateral RGC axon termination zone. Scale bars: 100 µm.

As the Nell2 gene encodes a secreted protein, the Nell2 protein could, in principle, diffuse to the outside of the ipsilateral territory. To examine whether this is the case, we determined the Nell2 distribution in the dLGN by immunohistochemistry using anti-Nell2 antibody (Jiang et al., 2009). As shown in Fig. 1E, the pattern of Nell2 protein distribution was very similar to that of Nell2 RNA expression, indicating that most of the secreted Nell2 protein remains in the region of its origin. Taken together, these results indicate that Nell2 (RNA and protein) is expressed and localized in the termination area of ipsilateral RGC axons in the developing dLGN.

Nell2-null mice have defects in the eye-specific retinogeniculate projection

To determine whether Nell2 is involved in development of the eye-specific projection, we examined the retinogeniculate projection in *Nell2*$^{-/-}$ mice (Matsuyama et al., 2004; Nakamoto et al., 2014). Overall structure and cytoarchitecture of the visual system (retina, optic chiasm and dLGN) are maintained in the mutant mice (Figs 2 and 3). We labelled the whole eyes with an axon tracer dye of two different colours, and the location of the projection from each eye was examined in the dLGN (Bjartmar et al., 2006; Huberman et al., 2002). In normal development, retinal projections from the two eyes are largely intermixed with each other at P4, but by P12 they are well segregated and resemble the pattern found in the adult (Guido, 2008; Rossi et al., 2001) (Fig. 2A, Fig. S2A,C). In *Nell2*$^{-/-}$ mice, termination zones of contra- and ipsilateral RGC axons in the dLGN were also significantly overlapped at P4 (Fig. S2B). At P10 and P12, contralateral and ipsilateral RGC axons in wild-type mice terminated in two non-overlapping domains: ipsilateral axons were confined to a small single patch located in the dorsomedial part of the dLGN, whereas contralateral axons terminated in the surrounding areas (Rossi et al., 2001) (Fig. 2A, Fig. S2C). In contrast, in *Nell2*$^{-/-}$ mice, contralateral axons invaded the ipsilateral territory of the dLGN, and ipsilateral axons terminated in partially fragmented patches, forming a mosaic pattern of contralateral and ipsilateral axon termination zones (Fig. 2B-D, Figs S2D and S3). At P12, aberrant invasion of the ipsilateral territory by contralateral axons was observed in 10/12 (83.3%) of *Nell2*$^{-/-}$ mice, but not in wild-type (0/10) mice (P<0.001). Although contralateral and ipsilateral axons terminated in aberrant locations of the dLGN, the segregation of inputs from the right and left eyes occurred properly (Fig. 2E and Fig. S4). These results indicate that Nell2 is essential for eye-specific targeting of RGC axons but not for segregation of retinal inputs in the dLGN.

Nell2-null mice show no obvious defects in RGC axon pathfinding

It is possible that the aberrant termination patterns observed in *Nell2*$^{-/-}$ dLGN were caused by misrouting of RGC axons at the optic chiasm. Axons that normally remain ipsilateral might instead cross the midline and project to the corresponding 'ipsilateral' territory in the contralateral dLGN, resulting in invasion of the ipsilateral domain by axons from the contralateral eye. If this were the case, there would be a decreased number of axons from the individual eyes that project to the ipsilateral dLGN. We therefore compared the ratio of termination zone of ipsilaterally projecting axons to total dLGN area. No significant difference was observed in the size of the ipsilateral patch between the wild-type and *Nell2*$^{-/-}$

Development (2019) 146, dev170704. doi:10.1242/dev.170704

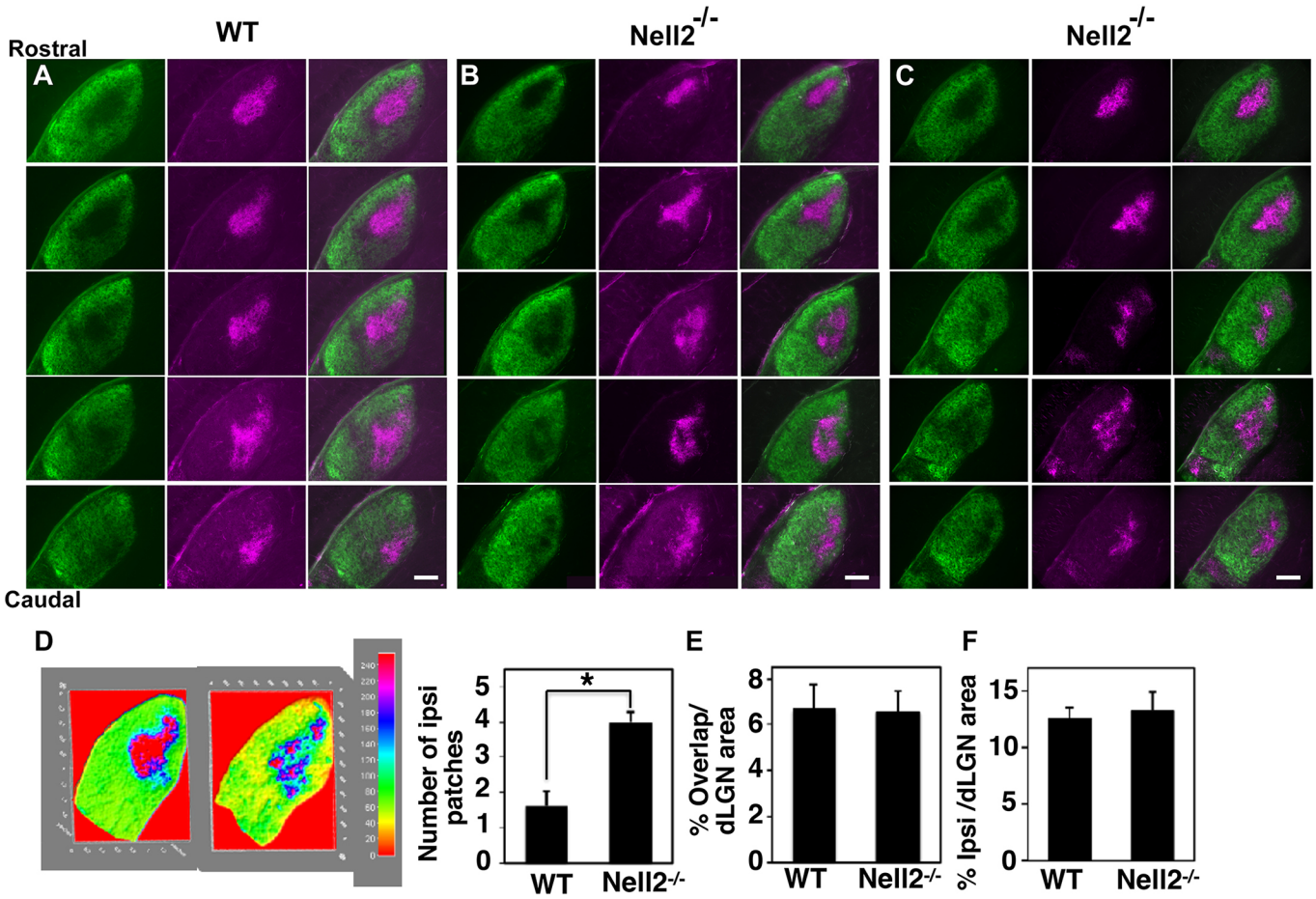

Fig. 2. Defects in the eye-specific retinogeniculate projection in *Nell2*$^{-/-}$ mice. (A-C) RGC axons of the right and left eyes were labelled at P9 by injection with cholera toxin B (CTB)-Alexa Fluor 488 (green) and CTB-Alexa Fluor 594 (magenta), respectively. Serial coronal sections through the left dLGN prepared at P12 are shown. In each panel, dorsal is at the top and lateral is on the left. (A) In the wild type (n=10), ipsilateral axons (magenta) are confined to a single patch in a dorsomedial region of the dLGN, and contralateral axons (green) terminate in the surrounding areas. (B,C) Two representative examples of the retinogeniculate projection in *Nell2*$^{-/-}$ mice (n=12). Contralateral axons invade the ipsilateral territory, forming a mosaic pattern of contralateral and ipsilateral axons (in 10/12 mice). Scale bars: 100 µm. (D) Quantification of the number of ipsilateral patches. The ipsilateral projection in *Nell2*$^{-/-}$ mice appeared patchy compared with that in wild-type mice. (E) Contralateral and ipsilateral axon overlap was quantified and is presented as the percentage of the total dLGN area containing overlap. (F) Quantification of the ratio of percent ipsilateral projection area to total dLGN area. In D-F, data are plotted as mean±s.e.m. *P<0.0001.

mice (Fig. 2F and Fig. S5). We also prepared sections through the optic chiasm region and examined patterns of RGC axon routing in *Nell2*$^{-/-}$ mice. No obvious defects were observed in the decussation pattern or structure of the optic chiasm, and fasciculation of RGC axons also appeared normal in *Nell2*$^{-/-}$ mice (Fig. 3). These results suggest that *Nell2*$^{-/-}$ mice have no obvious defects in RGC axon pathfinding.

Nell2 inhibits contralateral, but not ipsilateral, RGC axons *in vitro*

The Nell2 expression domain in the dLGN overlaps with the termination zone of ipsilateral RGC axons, which contralateral axons normally avoid (Fig. 1). In addition, we have previously demonstrated that Nell2 (Nel) inhibits axon outgrowth and induces growth cone collapse and axon retraction in RGCs of the chick (Jiang et al., 2009; Nakamura et al., 2012), in which all the mature RGCs send their projections contralaterally (Thanos and Bonhoeffer, 1984). These findings may suggest that Nell2 acts as an inhibitory guidance cue for contralateral RGC axons and prevents them from terminating in the ipsilateral territory of the dLGN. We therefore examined the effects of Nell2 on contralateral and ipsilateral RGC axons by using several axon behaviour assays *in vitro*.

We first tested effects of Nell2 on RGC axon outgrowth, using retinal explants prepared from the ventrotemporal (VT, containing ipsilaterally projecting RGCs) and ventronasal (VN, contralaterally projecting RGCs) retinae. VT and VN explants were individually cultured on the substratum coated with either a Nell2 protein conjugated with an alkaline phosphatase (AP) tag (Nell2-AP) or a control unconjugated AP. We found that Nell2 specifically inhibited outgrowth of RGC axons from VN explants (Fig. 4A-E). These results indicate that Nell2 inhibits outgrowth of contralateral RGC axons.

The ability to induce growth cone collapse is a hallmark of many inhibitory axon guidance cues, such as ephrins, slits and semaphorins. Therefore, we next examined how Nell2 regulates growth cone morphology of RGC axons. We cultured VT and VN retinal explants on a permissive substratum to allow formation of well-developed growth cones at the tip of RGC axons. The axons were then treated with Nell2-AP or AP, and their effects on morphology of growth cones were observed. Treatment with control AP did not affect the growth cone morphology in VT or VN axons. In contrast, Nell2-AP induced growth cone collapse in most VN, but not VT, axons (Fig. 4F-J). As we previously observed in the chick, Nell2-AP exerted growth cone collapsing effects on mouse

Development (2019) 146, dev170704. doi:10.1242/dev.170704

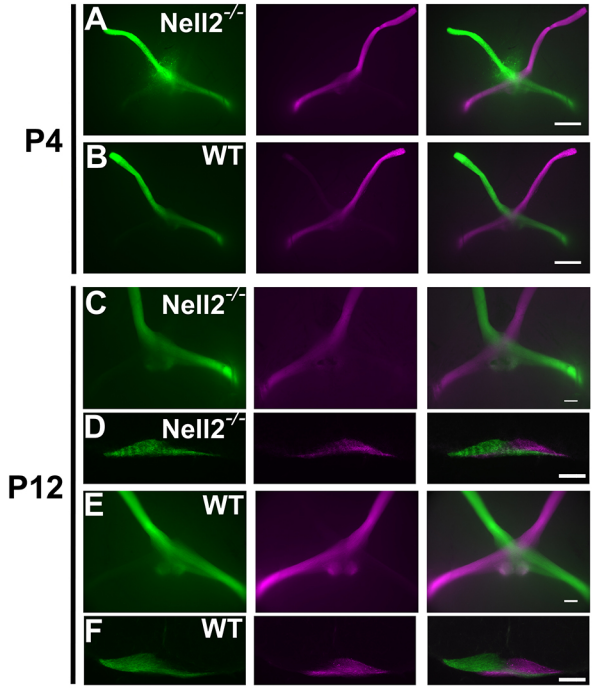

Fig. 3. No obvious defects in the decussation patterns at the optic chiasm of *Nell2*$^{-/-}$ mice. (A-F) RGC axons of the right and left eyes were labelled by injection with cholera toxin B (CTB)-Alexa Fluor 488 (green) and CTB-Alexa Fluor 594 (magenta), respectively. The brain was dissected out 3 days later, and decussation patterns of the optic nerve at the optic chiasm were observed in whole-mount preparations (A-C,E; ventral views, rostral is at the top) and in coronal sections (D,F; dorsal is at the top). (A) P4 *Nell2*$^{-/-}$ (n=8), (B) P4 wild type (n=5), (C,D) P12 *Nell2*$^{-/-}$ (n=6) and (E,F) P12 wild type (n=4). Scale bars: 100 µm.

RGC axons in a dose-dependent manner (Fig. S6). Our results indicate that Nell2 induces growth cone collapse specifically in contralaterally projecting RGC axons.

We then performed stripe assays (Hornberger et al., 1999) to examine whether contralateral and ipsilateral RGC axons show preference for or against Nell2. VT and VN explants were cultured on the substratum consisting of alternative stripes of Nell2-AP and AP, and thus RGC axons were given the choice of growing on Nell2-AP- or AP-containing substratum. As shown in Fig. 5, axons from VN axons prefer to grow on control AP stripes, whereas VT axons did not show preferences and grew randomly. Taken together, these *in vitro* experiments demonstrated that Nell2 acts as a contralateral RGC axon-specific inhibitory guidance cue.

Deletion of endogenous Nell2 in RGCs does not affect contralateral axon-specific inhibition caused by exogenous Nell2

It has previously been reported that Nell2 is expressed in developing RGCs (Nakamoto et al., 2014; Nelson et al., 2002; Wang et al., 2007). Therefore, it is possible that deletion of Nell2 in RGCs, rather than in the dLGN, contributed to the aberrant patterns of the retinogeniculate projection observed in *Nell2*$^{-/-}$ mice. For example, Nell2 might be expressed specifically in contra- or ipsilaterally projecting RGCs, and play roles in axon targeting in the dLGN in a cell-autonomous fashion. As shown in Fig. 6, however, Nell2 expression in RGCs was detected throughout the retina, and its expression domain extends to the retinal periphery, including the ventrotemporal region that contains Zic2-positive, ipsilaterally projecting RGCs. No obvious gradient of Nell2 expression was observed in the retina. The expression pattern of Nell2 in the retina therefore does not appear to correlate with a particular retinogeniculate projection phenotype.

We next examined whether removal of endogenous Nell2 in RGCs would alter responses of their axons to exogenous Nell2. We tested this by performing axon outgrowth assays and growth cone collapse assays using retinal explants prepared from *Nell2*$^{-/-}$ mice. When *Nell2*$^{-/-}$ retinal explants were cultured on Nell2-AP containing substratum, the outgrowth of VN, but not of VT, axons was significantly inhibited (Fig. 7A-E). Similarly, exogenous Nell2 induced growth cone collapse specifically in axons from VN retinal explants (Fig. 7F-J). These results indicate that when endogenous Nell2 is deleted in RGCs, exogenous Nell2 still exerts contralateral axon-specific inhibitory effects. Our findings suggest that the aberrant retinogeniculate projection patterns observed in *Nell2*$^{-/-}$ mice were caused by deletion of Nell2 expression in the dLGN, rather than in RGCs.

DISCUSSION

It has long been postulated that the eye-specific visual projection is regulated by layer- or domain-specific guidance cues; however, their molecular nature has remained elusive. The current study has indicated that Nell2 acts as a positional label for the territory of the dLGN where ipsilateral RGC axons terminate and contralateral axons normally avoid, and is essential for establishment of the eye-specific retinogeniculate projection.

At the time of retinogeniculate projection, Nell2 RNA is specifically detected in the ipsilateral domain, and although Nell2 is a secreted protein, immunohistological studies indicated that most of the Nell2 protein remains within the area of its origin. This finding is consistent with our previous observation in the chick that Nell2 (Nel) RNA expression and its protein distribution show similar layer-specific patterns in the developing chicken optic tectum (Jiang et al., 2009). The limited diffusion of Nell2 protein may be due to its heparin-binding activity through the N-terminus thrombospondin-like domain (Nakamura et al., 2012), and the Nell2 protein may be trapped *in situ* by heparin sulfate proteoglycans soon after secretion from Nell2-expressing cells.

Our *in vivo* axon tracing experiments indicated that, in *Nell2*$^{-/-}$ mice, contralateral RGC axons aberrantly invaded the ipsilateral domain of the dLGN. In a series of *in vitro* axon behaviour assays, Nell2 exerted inhibitory effects specifically on contralateral RGC axons: treatment with Nell2 caused axon outgrowth inhibition, growth cone collapse and axon repulsion in contralateral, but not ipsilateral, RGCs. Nell2 induced similar responses in both wild-type and *Nell2*$^{-/-}$ RGC axons, indicating that removal of endogenous Nell2 in RGCs does not affect the contralateral axon-specific inhibition caused by exogenous Nell2. The effects of Nell2 on contralateral RGC axons in the dLGN or *in vitro* are consistent with the model in which Nell2 in the ipsilateral domain of the dLGN acts as an inhibitory guidance cue specific for contralateral RGC axons and prevents them from entering the ipsilateral territory. The removal of the repellent Nell2 in the dLGN allows contralateral axons to invade and arborize ectopically in the ipsilateral domain (Fig. 8). Those results are also in agreement with our previous observation in the chick that Nell2 (Nel) inhibits RGC axons (which are all contralaterally projecting) and is expressed in specific tectal layers that (contralateral) RGC axons do not normally invade (Jiang et al., 2009; Nakamura et al., 2012).

Whereas the expression patterns of Nell2 in the developing mouse dLGN do not show obvious gradients, positional labels expressed in gradients across the projecting and target areas play key

Development (2019) 146, dev170704. doi:10.1242/dev.170704

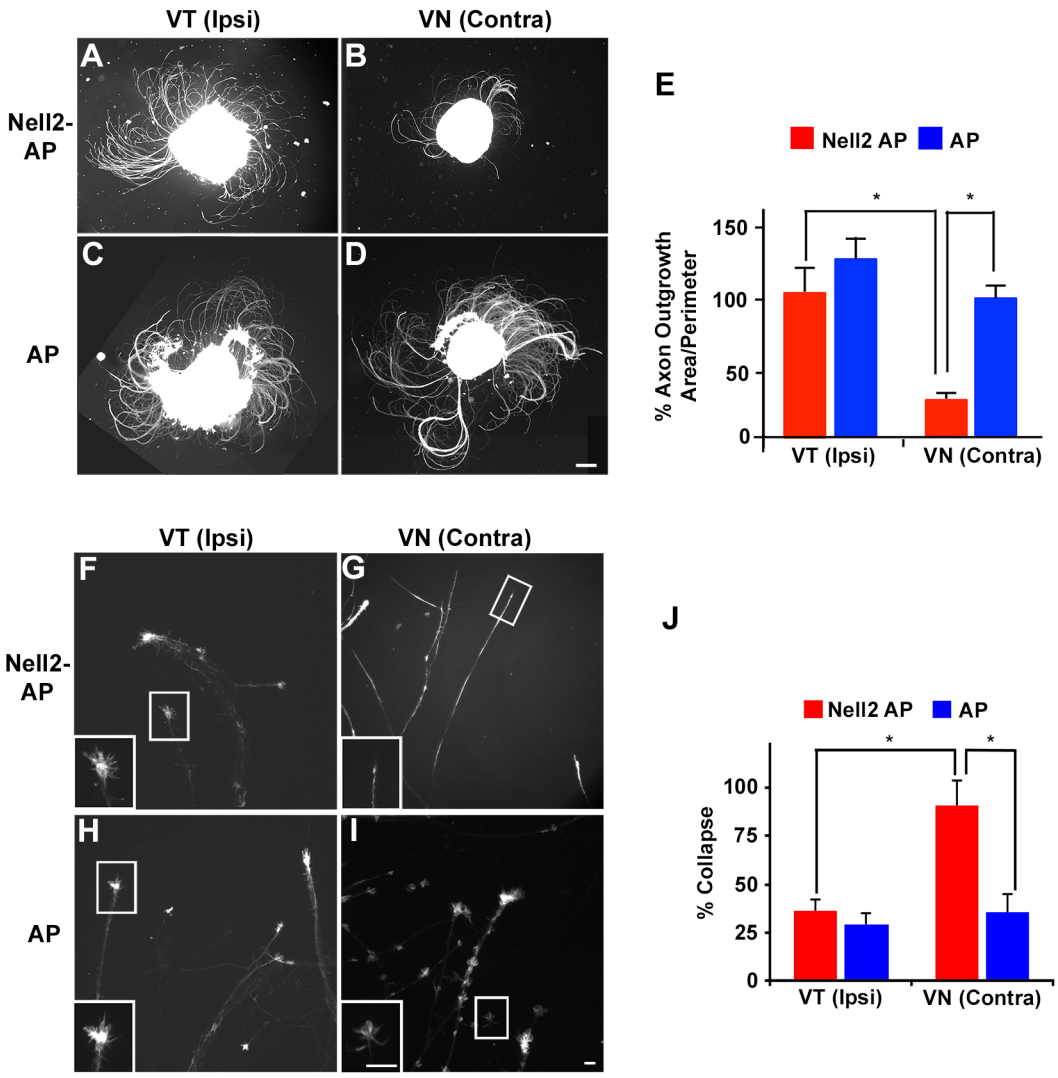

Fig. 4. Nell2 inhibits axon outgrowth and induces growth cone collapse specifically in contralaterally projecting RGCs. (A-E) Axon outgrowth assays. Explants of the ventrotemporal (VT; containing ipsilaterally projecting RGCs) (A,C) and ventronasal (VN; contralaterally projecting RGCs) (B,D) retina were prepared from E15.5 mouse embryos and cultured for 72 h on a substratum coated with Nell2-AP (A,B) or AP (C,D), and axon outgrowth was quantified (E) (n=4 for each condition). Nell2-AP significantly inhibited outgrowth of VN retinal axons. (F-J) Growth cone collapse assays. VT (F,H) and VN (G,I) retinal explants prepared from E15.5 mouse embryos were cultured *in vitro* for 48-72 h and then treated with Nell2-AP (F,G) or AP (H,I) (n=4 for each condition, at least 30 growth cones were observed in each experiment). The growth cone morphology was observed 30 min later. Higher-magnification views of representative growth cone morphology (boxed areas) are shown in the insets. (J) Quantification of the growth cone collapsing activity. The percentage of collapsed growth cones is plotted as mean±s.e.m. Nell2-AP induced growth cone collapse in VN but not in VT retinal axons. Scale bars: 100 µm in D; 25 µm in I. *P<0.001.

roles in topographic neural map formation (Flanagan, 2006). Ephrin A proteins are expressed in gradients in the dLGN (high in ventral-lateral-anterior and low in dorsal-medial-posterior) and, through interactions with EphA receptors expressed in complementary gradients in the retina (high in temporal, low in nasal), regulate formation of topographic mapping along the nasotemporal axis in the retina onto the dLGN and superior colliculus/optic tectum (Drescher et al., 1995; Feldheim et al., 2004, 1998; Nakamoto et al., 1996). Interestingly, ephrin A proteins have also been implicated in eye-specific axon targeting in the dLGN of the mouse (Pfeiffenberger et al., 2005) and ferret (Huberman et al., 2005). Similarly, the cell-surface adhesion molecule teneurin 3 is expressed in corresponding gradients in the dLGN (high in dorsal, low in ventral) and the retina (high in ventral, low in dorsal), and regulates the eye-specific patterning of the retinogeniculate projection through homophilic interactions (Leamey et al., 2007). Considering that the ipsilaterally projecting RGCs localize in the ventrotemporal region in the retina, it seems plausible that the key contributing factors in ephrin A- and teneurin 3-mediated patterning of eye-specific retinogeniculate projections are the nasal-retina versus temporal-retina distinction and the ventral-retina versus dorsal-retina distinction, respectively (Huberman et al., 2005). In contrast, our results in this study suggest that Nell2 contributes to establish the eye-specific projection patterns by using the contralateral-retina versus ipsilateral-retina distinction.

It is noteworthy that deletion of Nell2 also affected ipsilateral RGC axons in the dLGN. In *Nell2*$^{-/-}$ mice, subsets of ipsilateral axons appeared to be displaced from the ipsilateral domain and to terminate in partially fragmented patches in the dLGN. This phenotype could not be simply explained by inhibitory effects of Nell2 on contralateral axons alone. One model that could account for the behaviour of ipsilateral axons in the *Nell2*$^{-/-}$ dLGN involves

Development (2019) 146, dev170704. doi:10.1242/dev.170704

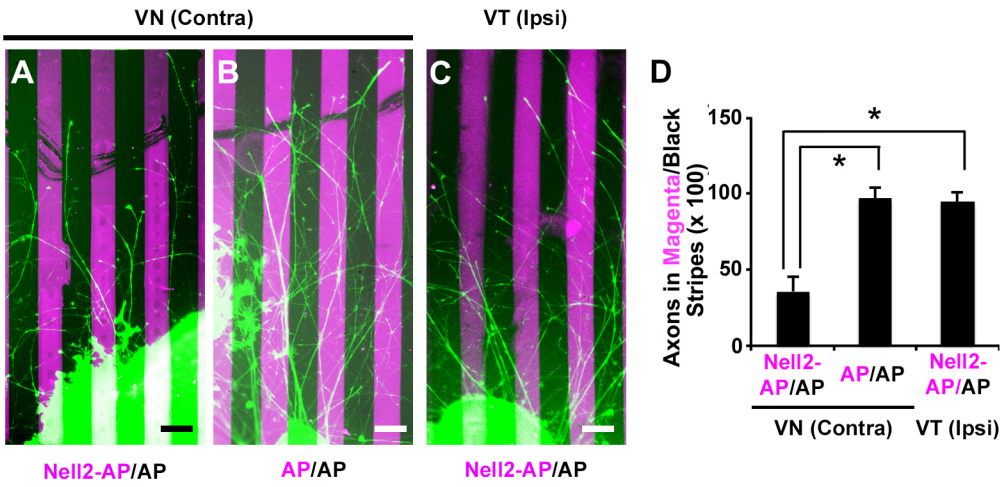

Fig. 5. Specific repulsion of contralaterally projecting RGC axons by Nell2. VN (A,B) and VT (C) retinal axons were grown on alternating stripes consisting of Nell2-AP- (A,C) or AP- (B) containing substrata [labelled with fluorescent microspheres (magenta)] and AP-containing substrata (black). Patterns of axon outgrowth were observed 48-72 h later. VN axons show a preference for control AP stripes, whereas VT axons show no preference. (D) Quantification of axon behaviour on Nell2 stripes. Data are mean±s.e.m. n=6 for each experimental condition. Scale bars: 100 µm. *P<0.001.

axon-axon competition, in combination with contralateral axon-specific repulsion by Nell2. It is thought that, during development, axons compete with one another to fill available space in the target region (Holt and Harris, 1993; Jacobson and Rao, 2005). In normal development, by acting as a repellent for contralateral RGC axons, Nell2 would bias this competition and give ipsilateral axons an advantage in the Nell2-containing ipsilateral domain: contralateral RGC axons are repelled by Nell2 in the ipsilateral domain, and thus they would be forced to terminate in the surrounding contralateral territory; whereas ipsilateral axons are not repelled by Nell2 and can terminate in the ipsilateral domain. Ipsilateral axons do not terminate in the contralateral domain because there is greater axon-axon competition, so they prefer to avoid this competition and arborize only in the ipsilateral domain. In *Nell2*$^{-/-}$ mice, the Nell2 repellent is removed, and thus contralateral axons are now able to invade the ipsilateral domain and compete more effectively with ipsilateral axons there. Ipsilateral axons face increased competition in the ipsilateral domain, and subsets of the ipsilateral axons lose competition and spread out into surrounding areas in the contralateral domain. The model thus seems to fit well with the phenotypes of contra- and ipsilateral RGC axons in *Nell2*$^{-/-}$ mice observed in this study. Similar repulsion/competition models in which axon-axon competition is biased by non-uniform expression of guidance molecules in the target region were proposed to explain the aberrant projection patterns of nasal RGC axons in ephrin A mutant mice (Feldheim et al., 2000, 1998).

Despite the aberrant patterns of contra- and ipsilateral axon termination, inputs from the right and left eyes are still segregated, suggesting that Nell2 is required for proper placement of eye-specific inputs in the dLGN but is not essential for segregation of those inputs. Similar results have been previously reported for ephrin As: gradients of ephrin As in the dLGN are required for the proper placement of contra- and ipsilateral inputs but not required for their segregations (Pfeiffenberger et al., 2005). Taken together, those findings indicate differential and complementary contributions of activity-dependent and activity-independent mechanisms to the establishment of the eye-specific retinogeniculate projection.

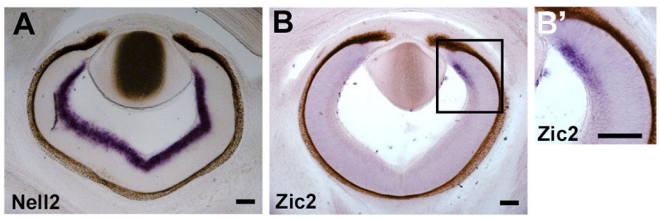

Fig. 6. Nell2 is expressed in both contra- and ipsilaterally projecting RGCs. Horizontal sections across the ventral retina were prepared from wild-type mouse embryos at E15.5 and hybridized with an RNA probe for Nell2 (A) or Zic2 (B). A higher-magnification view of the area outlined by the black rectangle in B is shown in (B′). Nell2 is expressed in RGCs throughout the retina, and its expression domain extends to the periphery of the retina, including the expression domain of Zic2, which is specifically expressed in ipsilaterally projecting RGCs in the ventrotemporal retina. Scale bars: 200 µm.

Recently, Nell2 has been shown to repel murine spinal commissural axons through the Robo3 receptor and steer them towards and across the midline of the spinal cord (Jaworski et al., 2015). In the developing mouse retina, however, Robo3 is not expressed in RGCs (Blackshaw et al., 2004), and expression of related Robo2 and Robo1 are detected throughout the RGC layer (Robo2 is expressed in most cells and Robo1 in a scattered subpopulation of cells in the RGC layer); this does not correlate with a particular retinogeniculate projection phenotype (Erskine et al., 2000). Therefore, it seems unlikely that Robo receptors are responsible for the Nell2-medicated eye-specific retinogeniculate projection. In addition, whereas EGF-like repeats of the Nell2 protein appear to be responsible for repulsion of spinal commissural axons (Jaworski et al., 2015), our previous studies have revealed that cysteine-rich domains exert inhibition of retinal axons (Nakamoto et al., 2014). These findings suggest that Nell2 regulates behaviour of retinal and spinal commissural axons through its different domains binding to distinct cognate receptors. Interestingly, it has been shown that different receptors mediate VEGFA-induced attraction in RGC axons (the NRP1 receptor) and spinal commissural axons [the FLK1 (KDR/VEGFR2) receptor] (Erskine et al., 2011; Ruiz de Almodovar et al., 2011). In view of the structural similarities between Nell2 and thrombospondin 1, it seems likely that Nell2 interacts with a diverse range of cell-surface molecules using different domains. Identification of functional Nell2 receptors for RGC axon guidance will be required to fully understand signalling mechanisms for Nell2-mediated eye-specific visual projection.

MATERIALS AND METHODS

Nell2 mutant mice and genotyping

Mutant mice carrying the Nell2-null allele have been described previously (Matsuyama et al., 2004) and were maintained on a C57BL/6 background in the Medical Research Facility at the University of Aberdeen, UK. The animals were used under licenses from the UK Home Office in

Development (2019) 146, dev170704. doi:10.1242/dev.170704

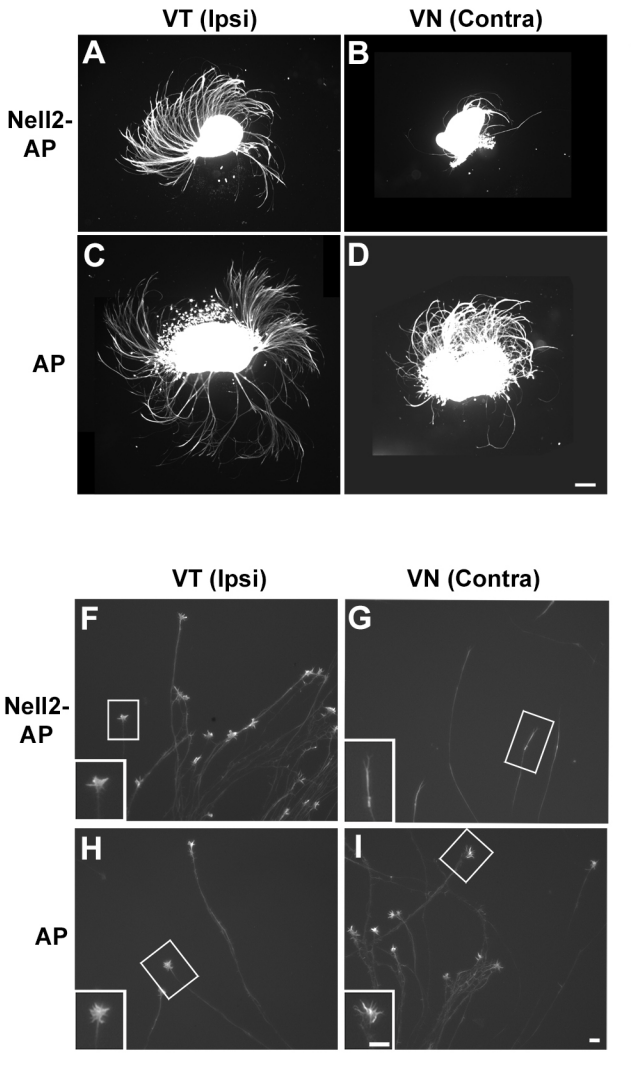

Fig. 7. Nell2 causes contralateral axon-specific inhibition in RGCs that lack endogenous Nell2. (A-E) Axon outgrowth assays. VT (A,C) and VN (B,D) retinal explants were prepared from *Nell2*$^{-/-}$ mouse embryos at E15.5, and cultured on a substratum coated with Nell2-AP (A,B) or AP (C,D). Axon outgrowth was quantified 72 h later (E) (*n*=4 for each condition). Nell2-AP significantly inhibited axon outgrowth from VN explants prepared from *Nell2*$^{-/-}$ mouse retinae. (F-J) Growth cone collapse assays. VT (F,H) and VN (G,I) retinal explants were prepared from *Nell2*$^{-/-}$ mouse embryos at E15.5, cultured *in vitro* for 48-72 h, and then treated with Nell2-AP (F,G) or AP (H,I) (*n*=4 for each condition, at least 30 growth cones were observed in each experiment). The growth cone morphology was observed 30 min later. Higher-magnification views of representative growth cone morphology (boxed areas) are shown in the insets. (J) Quantification of the growth cone collapsing activity. The percentage of collapsed growth cones was plotted as mean±s.e.m. Nell2-AP induced growth cone collapse in VN but not in VT retinal axons prepared from *Nell2*$^{-/-}$ mouse embryos. Scale bars: 100 µm in D; 25 µm in I. **P*<0.001.

accordance with the Animals (Scientific Procedures) Act 1986 and following approval from the University's Ethical Review Committee. For genotyping, genomic DNA was PCR amplified using primers 5′-ATGG-AATCCCGGGTGTTACT-3′ and 5′-CTCCCCAAGTTCTAACTCTG-3′ for the wild-type Nell2 locus, and 5′-ATGTATGGTGGTGGGAGGATG-C-3′ and 5′-GCCTTCTTGACGAGTTCTTCTGA-3′ for the mutant allele.

RNA *in situ* hybridization and immunohistochemistry

In situ RNA hybridization on 30-50 µm mouse brain sections was performed using digoxigenin-labelled probes for Nell2, as previously described (Nakamura et al., 2012). Immunohistochemistry was performed as previously described (Jiang et al., 2009; Nakamura et al., 2012) by using anti-Nell2 (Nel) antibody and Alexa Fluor 594-conjugated anti-rabbit IgG.

Retinal axon tracing

Mouse pups were anesthetized by isoflurane inhalation and received intravitreal injections of cholera toxin-B subunit (CTB) conjugated to Alexa Fluor 488 dye (green label) into one eye and CTB conjugated to Alexa Fluor 594 dye (red label) into the other eye (2-3 µl per eye; 0.5% in sterile saline; Invitrogen). Three days later, brains were dissected out, fixed with 4% paraformaldehyde overnight and embedded in 3% low melting point agarose (Sigma) in PBS. Then coronal sections (50 µm) were cut using a vibratome (Leica).

Images of retinal axon projections from the two eyes were captured using a CCD camera attached to a Zeiss fluorescent microscope with 10× and 20× objectives, and digitized independently using ImageJ. For quantification, only three sections that contained the largest ipsilateral projections were analysed (corresponding to the middle third of the LGN). To quantify eye-specific segregation and ipsilateral projection, the boundary of the dLGN was outlined, excluding the intrageniculate leaflet, the ventral LGN and the optic tract, and square pixels of the dLGN area were calculated. The pixel overlap between ipsilateral and contralateral projections, and the proportion of dLGN occupied by ipsilateral axons were measured as a pixel ratio to the dLGN region.

Axon outgrowth assays

Retinal explants were prepared from VT and VN areas of the E15.5 mouse retinae. The explants were cultured in the retinal culture medium (15% foetal bovine serum, 0.6% glucose, penicillin/streptomycin in DMEM:F12=1:1) in a four-well culture dish (Nunc) that had been pre-coated with 50 µg/ml of laminin and then with 0.25 µM of Nell2-AP or AP. After 72 h, axons were labelled by incubating the cultures in 33 µM carboxylfluorescein diacetate succinimidyl ester (Molecular Probes) for 5 min and photographed. For quantification of axon outgrowth, areas of axon growth were measured and normalized by the length of their perimeter using ImageJ.

Growth cone collapse assays

Growth cone collapse assays were performed essentially as described previously (Jiang et al., 2009; Nakamura et al., 2012). Retinal explants were prepared from E15.5 mouse embryos and cultured for 48-72 h on the substratum coated with 100 µg/ml laminin and in the retinal culture medium. Then retinal axons were treated with 0.25 µM Nell2-AP or control AP. The

Development (2019) 146, dev170704. doi:10.1242/dev.170704

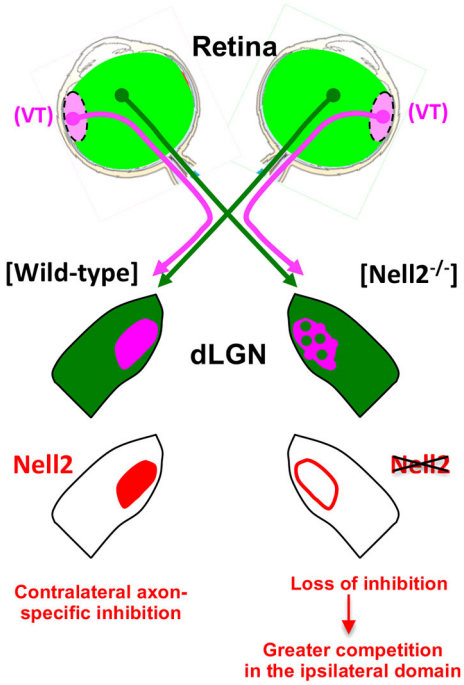

Fig. 8. Repulsion/competition model for the function of Nell2 in the eye-specific retinogeniculate projection. (Top) In the mouse visual system, the ipsilateral RGC axons (~3-5% of the optic nerve fibres) arise from a ventrotemporal (VT) segment of the retina. In the dLGN, ipsilateral axons are confined to a small single patch located in the dorsomedial part of the dLGN (magenta), whereas contralateral axons terminated in the surrounding areas (green). In *Nell2*$^{-/-}$ mice, contralateral RGC axons abnormally invade the ipsilateral domain, whereas ipsilateral axons terminated in partially fragmented patches, thus forming a mosaic pattern of contralateral and ipsilateral axon termination zones. (Bottom) Repulsion/competition model. Axons compete with one another for space in the target. The contralateral axon-specific repellent Nell2 (red) in the ipsilateral domain biases this competition. Contralateral RGC axons are repelled by Nell2, and thus they are forced to terminate in the surrounding contralateral domain, whereas ipsilateral axons can project to the ipsilateral domain. Ipsilateral axons do not terminate in the contralateral domain because there is greater axon-axon competition, so they prefer to avoid this competition and arborize only in the ipsilateral domain. In *Nell2*$^{-/-}$ mice, the Nell2-mediated repulsion is removed, and contralateral axons can now invade the ipsilateral domain and compete more effectively with ipsilateral axons there. Subsets of the ipsilateral axons lose competition and spread out into surrounding areas in the contralateral domain.

explants were incubated at 37°C for 30 min, fixed and stained with Alexa Fluor 488 phalloidin (Invitrogen). Individual growth cones were scored as collapsed or not collapsed, and percentages of collapsed growth cones were calculated. Growth cones that have three or more filopodia with obvious lamellipodia were classified as not collapsed. In each experiment, at least 30 growth cones for each condition were scored, and three independent experiments were performed.

Stripe assays

Stripe assays using purified Nell2-AP and unconjugated AP protein were performed as previously described (Knöll et al., 2007). Briefly, a silicon matrix with 90 µm channels [obtained from the laboratory of Prof. Martin Bastmeyer (Zoologisches Institut, Universität Karlsruhe, Germany)] was placed onto a 6 cm petri dish, then a first protein solution was applied (0.5 µM Nell2-AP or AP conjugated with Alexa Fluor 647) and the first stripes were set by incubating for 30 min at 37°C in a moist chamber. After rinsing the channels with HBSS, the matrix was removed. A second protein solution (0.5 µM AP) was applied to the stripe area, and the dishes were incubated for 30 min at 37°C. The second protein solution was then removed and the dishes were rinsed with HBSS. Then the stripes were coated with 20 µg/ml laminin (Invitrogen) in HBSS for 2 h at 37°C in a moist chamber, and rinsed with HBSS. Retinal explants prepared from E15.5 mouse embryos were cultured on the stripes in the retinal culture medium for ~2-3 days. Axons were stained with Alexa Fluor 488 phalloidin. To generate a quantitative index of RGC axon growth on membrane stripes, the integrated fluorescent signals from the axons in the first stripes versus those in the second stripes was calculated for a rectangular region of interest that spanned the width of the image adjacent to the explant edge using ImageJ (Stettler et al., 2012).

Statistical analysis

For statistical analysis of the retinogeniculate projection patterns in *Nell2* mutant mice, an unpaired Student's *t*-test was used. Results of the *in vitro* axon behaviour assays were analysed by ANOVA. *P* values are given in the figure legends. No statistical methods were used to predetermine the sample sizes, but our sample sizes are similar to those generally employed in the field. Part of the data collection and analyses were performed blind to the conditions of the experiments.

Acknowledgements

We thank Lynda Erskine, Colin McCaig and David Feldheim for discussion and comments on the manuscript; the Imaging Core Facility of the Institute of Medical Sciences and the Medical Research Facility of University of Aberdeen for technical support.

Competing interests

The authors declare no competing or financial interests.

Author contributions

Conceptualization: C.N., M.N.; Methodology: C.N., M.N.; Software: C.N., M.N.; Validation: C.N., M.N.; Formal analysis: C.N., M.N.; Investigation: C.N., E.D., M.N.; Resources: C.N., M.H., M.N.; Data curation: C.N., M.N.; Writing - original draft: C.N., M.N.; Writing - review & editing: C.N., E.D., M.H., M.N.; Visualization: C.N., M.N.; Supervision: C.N., M.N.; Project administration: M.N.; Funding acquisition: M.N.

Funding

This work was supported by grants from Biotechnology and Biological Sciences Research Council (BB/G007632/1) and the Royal Society (to M.N.).

Supplementary information

Supplementary information available online at
http://dev.biologists.org/lookup/doi/10.1242/dev.170704.supplemental

References

Bjartmar, L., Huberman, A. D., Ullian, E. M., Renteria, R. C., Liu, X., Xu, W., Prezioso, J., Susman, M. W., Stellwagen, D., Stokes, C. C. et al. (2006). Neuronal pentraxins mediate synaptic refinement in the developing visual system. *J. Neurosci.* **26**, 6269-6281.

Blackshaw, S., Harpavat, S., Trimarchi, J., Cai, L., Huang, H., Kuo, W. P., Weber, G., Lee, K., Fraioli, R. E., Cho, S. H. et al. (2004). Genomic analysis of mouse retinal development. *PLoS Biol.* **2**, E247.

Chapman, B. (2000). Necessity for afferent activity to maintain eye-specific segregation in ferret lateral geniculate nucleus. *Science* **287**, 2479-2482.

Crowley, J. C. and Katz, L. C. (1999). Development of ocular dominance columns in the absence of retinal input. *Nat. Neurosci.* **2**, 1125-1130.

Drescher, U., Kremoser, C., Handwerker, C., Loschinger, J., Noda, M. and Bonhoeffer, F. (1995). In vitro guidance of retinal ganglion cell axons by RAGS, a 25 kDa tectal protein related to ligands for Eph receptor tyrosine kinases. *Cell* **82**, 359-370.

Erskine, L. and Herrera, E. (2014). Connecting the retina to the brain. *ASN Neuro* **6**.

Erskine, L., Williams, S. E., Brose, K., Kidd, T., Rachel, R. A., Goodman, C. S., Tessier-Lavigne, M. and Mason, C. A. (2000). Retinal ganglion cell axon guidance in the mouse optic chiasm: expression and function of robos and slits. *J. Neurosci.* **20**, 4975-4982.

Erskine, L., Reijntjes, S., Pratt, T., Denti, L., Schwarz, Q., Vieira, J. M., Alakakone, B., Shewan, D. and Ruhrberg, C. (2011). VEGF signaling through neuropilin 1 guides commissural axon crossing at the optic chiasm. *Neuron* **70**, 951-965.

Feldheim, D. A., Vanderhaeghen, P., Hansen, M. J., Frisén, J., Lu, Q., Barbacid, M. and Flanagan, J. G. (1998). Topographic guidance labels in a sensory projection to the forebrain. *Neuron* **21**, 1303-1313.

Feldheim, D. A., Kim, Y.-I., Bergemann, A. D., Frisén, J., Barbacid, M. and Flanagan, J. G. (2000). Genetic analysis of ephrin-A2 and ephrin-A5 shows their requirement in multiple aspects of retinocollicular mapping. *Neuron* **25**, 563-574.

Feldheim, D. A., Nakamoto, M., Osterfield, M., Gale, N. W., DeChiara, T. M., Rohatgi, R., Yancopoulos, G. D. and Flanagan, J. G. (2004). Loss-of-function analysis of EphA receptors in retinotectal mapping. *J. Neurosci.* **24**, 2542-2550.
Flanagan, J. G. (2006). Neural map specification by gradients. *Curr. Opin. Neurobiol.* **16**, 59-66.
Garcia-Frigola, C. and Herrera, E. (2010). Zic2 regulates the expression of Sert to modulate eye-specific refinement at the visual targets. *EMBO J.* **29**, 3170-3183.
Godement, P., Salaün, J. and Imbert, M. (1984). Prenatal and postnatal development of retinogeniculate and retinocollicular projections in the mouse. *J. Comp. Neurol.* **230**, 552-575.
Guido, W. (2008). Refinement of the retinogeniculate pathway. *J. Physiol.* **586**, 4357-4362.
Heesy, C. P. (2004). On the relationship between orbit orientation and binocular visual field overlap in mammals. *Anat. Rec A Discov. Mol. Cell Evol. Biol.* **281**, 1104-1110.
Holt, C. E. and Harris, W. A. (1993). Position, guidance, and mapping in the developing visual system. *J. Neurobiol.* **24**, 1400-1422.
Hornberger, M. R., Dutting, D., Ciossek, T., Yamada, T., Handwerker, C., Lang, S., Weth, F., Huf, J., Wessel, R., Logan, C. et al. (1999). Modulation of EphA receptor function by coexpressed ephrinA ligands on retinal ganglion cell axons. *Neuron* **22**, 731-742.
Huberman, A. D. (2007). Mechanisms of eye-specific visual circuit development. *Curr. Opin. Neurobiol.* **17**, 73-80.
Huberman, A. D., Stellwagen, D. and Chapman, B. (2002). Decoupling eye-specific segregation from lamination in the lateral geniculate nucleus. *J. Neurosci.* **22**, 9419-9429.
Huberman, A. D., Murray, K. D., Warland, D. K., Feldheim, D. A. and Chapman, B. (2005). Ephrin-As mediate targeting of eye-specific projections to the lateral geniculate nucleus. *Nat. Neurosci.* **8**, 1013-1021.
Huberman, A. D., Feller, M. B. and Chapman, B. (2008). Mechanisms underlying development of visual maps and receptive fields. *Annu. Rev. Neurosci.* **31**, 479-509.
Huberman, A. D., Clandinin, T. R. and Baier, H. (2010). Molecular and cellular mechanisms of lamina-specific axon targeting. *Cold Spring Harb. Perspect Biol.* **2**, a001743.
Huh, G. S., Boulanger, L. M., Du, H., Riquelme, P. A., Brotz, T. M. and Shatz, C. J. (2000). Functional requirement for class I MHC in CNS development and plasticity. *Science* **290**, 2155-2159.
Jacobson, M. and Rao, M. S. (2005). *Developmental Neurobiology*, 4th edn. New York: Kluwer Academic/Plenum.
Jaworski, A., Tom, I., Tong, R. K., Gildea, H. K., Koch, A. W., Gonzalez, L. C. and Tessier-Lavigne, M. (2015). Operational redundancy in axon guidance through the multifunctional receptor Robo3 and its ligand NELL2. *Science* **350**, 961-965.
Jiang, Y., Obama, H., Kuan, S. L., Nakamura, R., Nakamoto, C., Ouyang, Z. and Nakamoto, M. (2009). In vitro guidance of retinal axons by a tectal lamina-specific glycoprotein Nel. *Mol. Cell. Neurosci.* **41**, 113-119.
Knöll, B., Weinl, C., Nordheim, A. and Bonhoeffer, F. (2007). Stripe assay to examine axonal guidance and cell migration. *Nat. Protoc.* **2**, 1216-1224.
Kuroda, S., Oyasu, M., Kawakami, M., Kanayama, N., Tanizawa, K., Saito, N., Abe, T., Matsuhashi, S. and Ting, K. (1999). Biochemical characterization and expression analysis of neural thrombospondin-1-like proteins NELL1 and NELL2. *Biochem. Biophys. Res. Commun.* **265**, 79-86.
Leamey, C. A., Merlin, S., Lattouf, P., Sawatari, A., Zhou, X., Demel, N., Glendining, K. A., Oohashi, T., Sur, M. and Fässler, R. (2007). Ten_m3 regulates eye-specific patterning in the mammalian visual pathway and is required for binocular vision. *PLoS Biol.* **5**, e241.
Matsuhashi, S., Noji, S., Koyama, E., Myokai, F., Ohuchi, H., Taniguchi, S. and Hori, K. (1995). New gene, nel, encoding a M(r) 93 K protein with EGF-like repeats is strongly expressed in neural tissues of early stage chick embryos. *Dev. Dyn.* **203**, 212-222.
Matsuhashi, S., Noji, S., Koyama, E., Myokai, F., Ohuchi, H., Taniguchi, S. and Hori, K. (1996). New gene, nel, encoding a Mr 91 K protein with EGF-like repeats is strongly expressed in neural tissues of early stage chick embryos. *Dev. Dyn.* **207**, 233-234.
Matsuyama, S., Aihara, K., Nishino, N., Takeda, S., Tanizawa, K., Kuroda, S. and Horie, M. (2004). Enhanced long-term potentiation in vivo in dentate gyrus of NELL2-deficient mice. *Neuroreport* **15**, 417-420.
Muir-Robinson, G., Hwang, B. J. and Feller, M. B. (2002). Retinogeniculate axons undergo eye-specific segregation in the absence of eye-specific layers. *J. Neurosci.* **22**, 5259-5264.
Nakamoto, M., Cheng, H.-J., Friedman, G. C., McLaughlin, T., Hansen, M. J., Yoon, C. H., O'Leary, D. D. and Flanagan, J. G. (1996). Topographically specific effects of ELF-1 on retinal axon guidance in vitro and retinal axon mapping in vivo. *Cell* **86**, 755-766.
Nakamoto, C., Kuan, S.-L., Findlay, A. S., Durward, E., Ouyang, Z., Zakrzewska, E. D., Endo, T. and Nakamoto, M. (2014). Nel positively regulates the genesis of retinal ganglion cells by promoting their differentiation and survival during development. *Mol. Biol. Cell* **25**, 234-244.
Nakamura, R., Nakamoto, C., Obama, H., Durward, E. and Nakamoto, M. (2012). Structure-function analysis of Nel, a thrombospondin-1-like glycoprotein involved in neural development and functions. *J. Biol. Chem.* **287**, 3282-3291.
Nelson, B. R., Matsuhashi, S. and Lefcort, F. (2002). Restricted neural epidermal growth factor-like like 2 (NELL2) expression during muscle and neuronal differentiation. *Mech. Dev.* **119** Suppl. 1, S11-S19.
Nelson, B. R., Claes, K., Todd, V., Chaverra, M. and Lefcort, F. (2004). NELL2 promotes motor and sensory neuron differentiation and stimulates mitogenesis in DRG in vivo. *Dev. Biol.* **270**, 322-335.
Newton, I. (1730). *Opticks or A Treatise of the Reflections, Refractions, Inflections & Colours of Light*, 4th edn. New York: Dover Publications, Inc.
Oyasu, M., Kuroda, S., Nakashita, M., Fujimiya, M., Kikkawa, U. and Saito, N. (2000). Immunocytochemical localization of a neuron-specific thrombospondin-1-like protein, NELL2: light and electron microscopic studies in the rat brain. *Brain Res. Mol. Brain Res.* **76**, 151-160.
Petros, T. J., Rebsam, A. and Mason, C. A. (2008). Retinal axon growth at the optic chiasm: to cross or not to cross. *Annu. Rev. Neurosci.* **31**, 295-315.
Pettigrew, J. D. (1986). The evolution of binocular vision. In *Vis. Neurosci* (ed. J. D. Pettigrew K. J. Sanderson and W. R. Levick), pp. 208-222. Cambridge: Cambridge University Press.
Pfeiffenberger, C., Cutforth, T., Woods, G., Yamada, J., Rentería, R. C., Copenhagen, D. R., Flanagan, J. G. and Feldheim, D. A. (2005). Ephrin-As and neural activity are required for eye-specific patterning during retinogeniculate mapping. *Nat. Neurosci.* **8**, 1022-1027.
Polyak, S. (1957). *The Vertebrate Visual System*. Chicago: University of Chicago Press.
Rossi, F. M., Pizzorusso, T., Porciatti, V., Marubio, L. M., Maffei, L. and Changeux, J.-P. (2001). Requirement of the nicotinic acetylcholine receptor beta 2 subunit for the anatomical and functional development of the visual system. *Proc. Natl. Acad. Sci. USA* **98**, 6453-6458.
Ruiz de Almodovar, C., Fabre, P. J., Knevels, E., Coulon, C., Segura, I., Haddick, P. C., Aerts, L., Delattin, N., Strasser, G., Oh, W.-J. et al. (2011). VEGF mediates commissural axon chemoattraction through its receptor Flk1. *Neuron* **70**, 966-978.
Shatz, C. J. (1996). Emergence of order in visual system development. *Proc. Natl. Acad. Sci. USA* **93**, 602-608.
Stettler, O., Joshi, R. L., Wizenmann, A., Reingruber, J., Holcman, D., Bouillot, C., Castagner, F., Prochiantz, A. and Moya, K. L. (2012). Engrailed homeoprotein recruits the adenosine A1 receptor to potentiate ephrin A5 function in retinal growth cones. *Development* **139**, 215-224.
Thanos, S. and Bonhoeffer, F. (1984). Development of the transient ipsilateral retinotectal projection in the chick embryo: a numerical fluorescence-microscopic analysis. *J. Comp. Neurol.* **224**, 407-414.
Wang, J. T., Kunzevitzky, N. J., Dugas, J. C., Cameron, M., Barres, B. A. and Goldberg, J. L. (2007). Disease gene candidates revealed by expression profiling of retinal ganglion cell development. *J. Neurosci.* **27**, 8593-8603.
Watanabe, T. K., Katagiri, T., Suzuki, M., Shimizu, F., Fujiwara, T., Kanemoto, N., Nakamura, Y., Hirai, Y., Maekawa, H. and Takahashi, E. (1996). Cloning and characterization of two novel human cDNAs (NELL1 and NELL2) encoding proteins with six EGF-like repeats. *Genomics* **38**, 273-276.
Wilks, T. A., Harvey, A. R. and Rodger, J. (2013). Seeing with two eyes: integration of binocular retinal projections in the brain. In *Functional Brain Mapping and the Endeavor to Understand the Working Brain* (ed. F. Signorelli and D. Chirchiglia), pp. 227-250. Rijecka, Croatia: InTech.

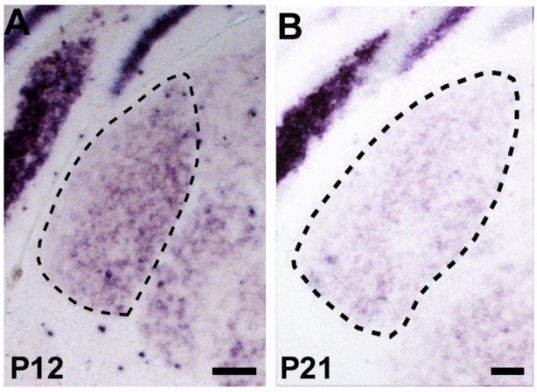

Fig. S1. Nell2 RNA expression in the dLGN at later stages of development Coronal sections through the dLGN were prepared from P12 (A) and P21 (B) wild type mice and subjected to RNA *in situ* hybridization with a probe for Nell2. Nell2 expression in the dLGN became decreased and diffused after P12. Dorsal is at the top, and lateral is on the left. Dotted lines indicate the boundary of dLGN. Scale bars, 100 μm.

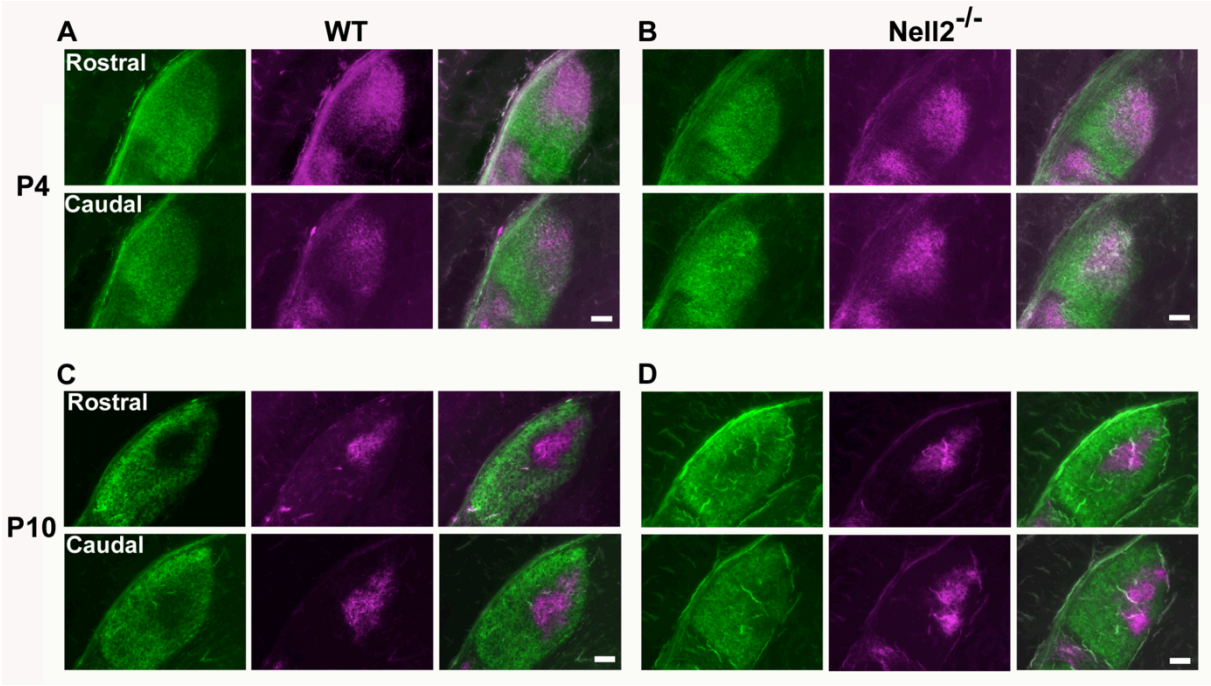

Fig. S2. Temporal analysis of eye-specific projection in wild type and Nell2$^{-/-}$ mice

The axon tracer dyes CTB-Alexa Fluor 488 (green) and CTB-Alexa Fluor 594 (magenta) were injected into the right and left eyes, respectively, at different postnatal stages. Three days later, serial coronal sections through the dLGN were prepared and projection patterns of RGC axons were examined. Projection patterns in the left dLGN are shown. (A, B) At P4, axons from the two eyes are significantly intermixed in both wild type (A (n=13)) and Nell2$^{-/-}$ mice (B (n=16)). (C, D) At P10, in the wild type (C (n=3)), ipsilateral axons (magenta) terminate in a single patch in the dorsomedial region of the dLGN, whereas contralateral axons (green) project to the surrounding areas. In Nell2$^{-/-}$ mice (D (n=5)), contralateral axons invade the ipsilateral territory, and termination zones of contralateral and ipsilateral axons show a mosaic pattern. In each panel, dorsal is at the top and lateral is on the left. Scale bars, 100 μm.

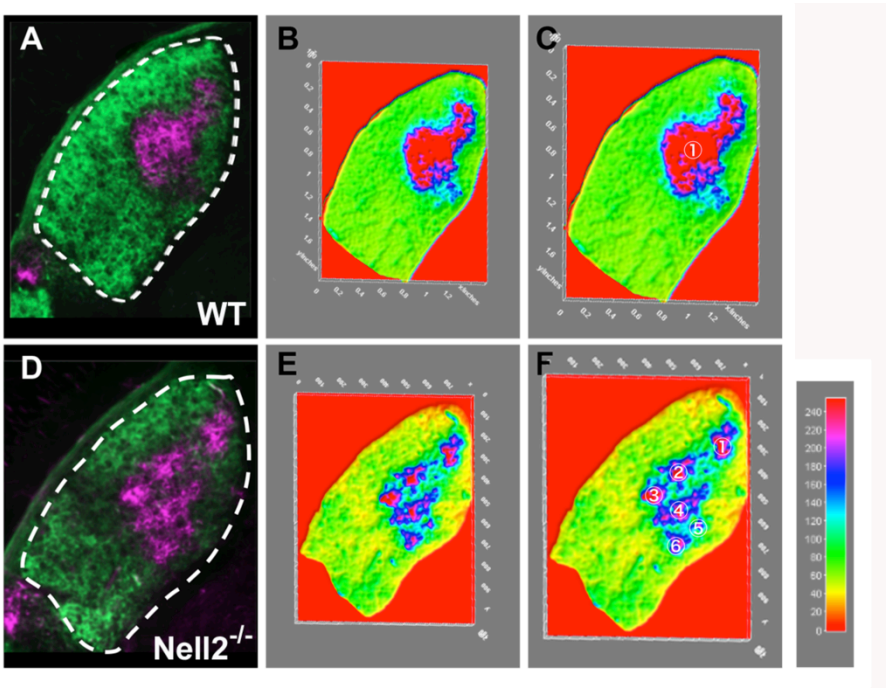

Fig. S3. Quantification of the number of ipsilateral patches in the dLGN RGC axons of the right and left eyes were labelled at P9 by injection with cholera toxin B (CTB)-Alexa Fluor 488 (green) and CTB-Alexa Fluor 594 (magenta), respectively. Coronal sections through the dLGN were prepared from wild-type (A-C) or Nell2$^{-/-}$ (D-F) mice at P12 and analysed. Images of the left dLGNs are shown. Distributions of ipsilateral axons were shown in colour-scaled densitometry plot by using ImageJ (B, E), and the number of the ipsilateral patches in each section was counted (C, F). In the wild type, ipsilateral axons are confined to a single patch in a dorsomedial region of the dLGN. In contrast, in NELL2$^{-/-}$ mice termination zones of ipsilateral axons are fragmented into multiple patches.

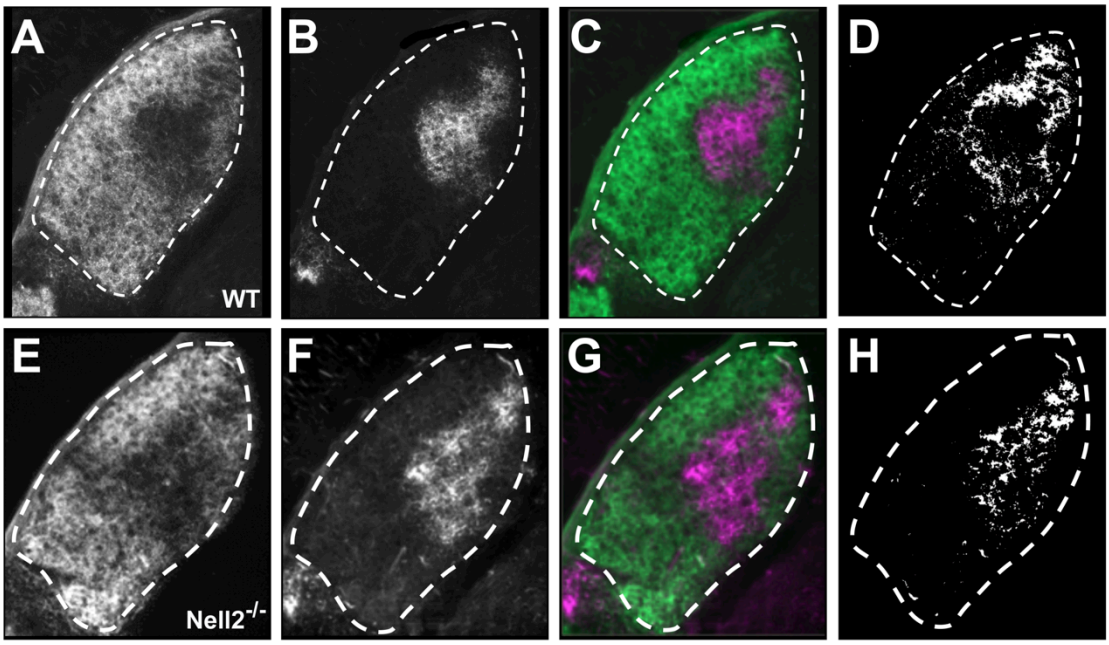

Fig. S4. Quantification of ipsilateral and contralateral axonal overlap in the dLGN

Pictures of contralateral projections (A, E), ipsilateral projections (B, F), merged images (C, G), and binary images representing ipsilateral and contralateral axonal overlap (D, H) at P12 are shown. To quantify ipsilateral and contralateral axon overlap, ImageJ was first used to reduce background with a rolling ball filter of 250 pixels. The dLGN area was then selected and isolated so that further manipulations were done only on this region. The ipsilateral and contralateral images of dLGN were then compared using the image calculator 'AND' function and the area of the resulting image was determined to be 'overlap'. The "overlap" image was thresholded and the square pixels of the area were measured using ImageJ. Percent overlap area was calculated by dividing the square pixels of overlap area (D, H) by those of total dLGN area using ImageJ measurement function. Dorsal is to the top, and lateral is to the left.

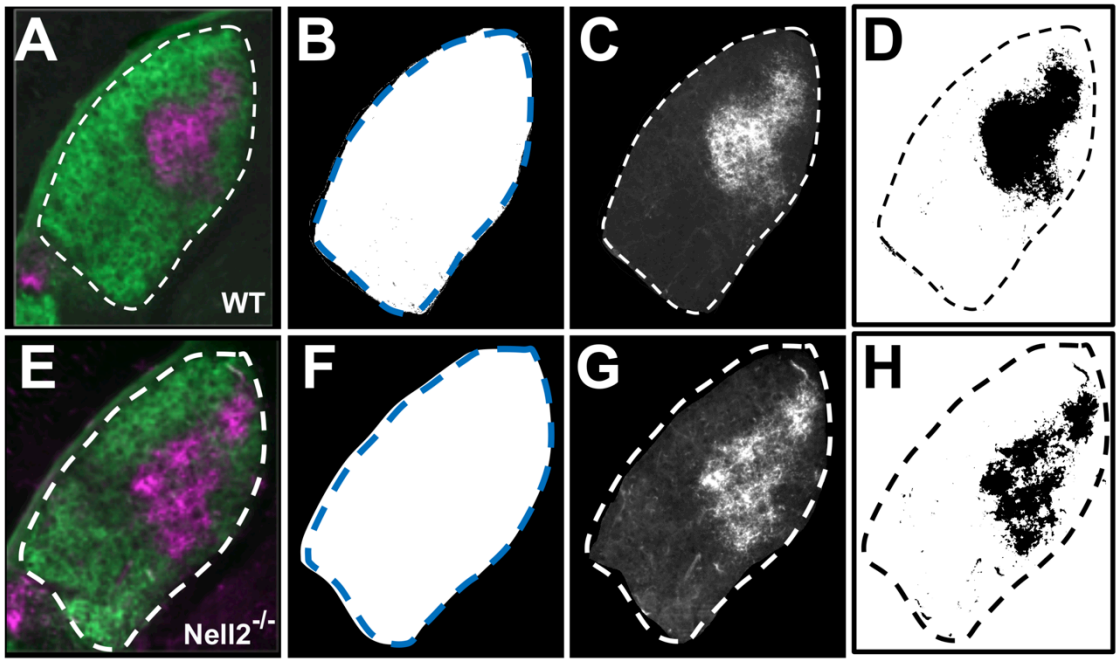

Fig. S5. Quantification of ipsilateral areas in the dLGN

(A, E) Contralateral (green) and ipsilateral (magenta) RGC projections in dLGN at P12. To quantify termination zones of ipsilateral RGC axons, the dLGN area was selected and isolated (B, F), and the images of ipsilateral RGC axon targeting in the dLGN (C, G) were thresholded (D, H). Percent ipsilateral areas were calculated by dividing square pixels of ipsilateral areas by those of dLGN areas, by using ImageJ measurement functions. Dorsal is to the top, lateral is to the left.

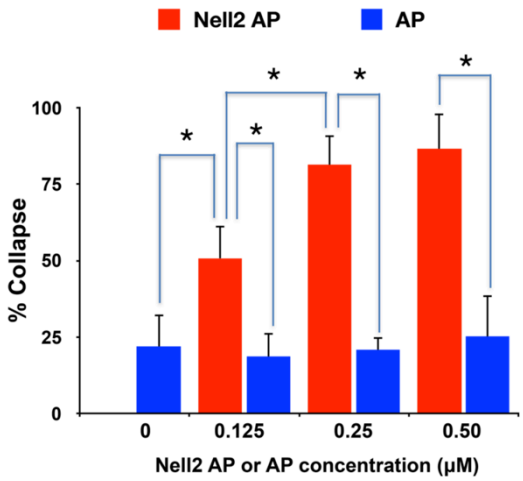

Fig. S6. Dose-dependent induction of growth cone collapse by Nell2 in contralaterally-projecting RGC axons

Explants prepared from a ventronasal part of the E15.5 mouse retina were cultured *in vitro* for 48-72 hours and then treated with different concentrations of Nell2-AP or AP (n=4 for each condition, 30< growth cones were observed in each experiment). The growth cone morphology was observed 30 min later. The percentage of collapsed growth cones was plotted as mean ± s.e.m. Nell2-AP induced growth cone collapse in ventronasal RGC axons in a dose-dependent manner. *, $p<0.001$.